

Apatite compositions and liquidus phase relationships on the join $\text{Ca}(\text{OH})_2\text{-CaF}_2\text{-Ca}_3(\text{PO}_4)_2\text{-H}_2\text{O}$ from 250 to 4000 bars

By G. M. BIGGAR, B.Sc., Ph.D.

Grant Institute of Geology, University of Edinburgh

[Read 8 June 1967]

Summary. Phase equilibria involving solids, liquids, and vapours on the join $\text{Ca}(\text{OH})_2\text{-CaF}_2\text{-Ca}_3(\text{PO}_4)_2\text{-H}_2\text{O}$ were determined at 1000 bars. The temperatures and liquid compositions (weight %) of the isobaric invariant reactions encountered were: portlandite + fluorite \rightarrow liquid, 687° C, 70 % $\text{Ca}(\text{OH})_2$ 30 % CaF_2 ; portlandite + fluorite + vapour \rightarrow liquid, 675° C, 69 % $\text{Ca}(\text{OH})_2$ 26 % CaF_2 5 % H_2O ; portlandite + fluorite + apatite \rightarrow liquid, 675° C, 73 % $\text{Ca}(\text{OH})_2$ 24 % CaF_2 3 % $\text{Ca}_3(\text{PO}_4)_2$; portlandite + fluorite + apatite + vapour \rightarrow liquid, 665° C, 70 % $\text{Ca}(\text{OH})_2$ 22 % CaF_2 3 % $\text{Ca}_3(\text{PO}_4)_2$ 5 % H_2O . The temperatures of these reactions were determined from over 400 experimental runs at selected pressures from 250 to 4000 bars. The composition of the apatite involved in the last two reactions was 60 % hydroxyapatite 40 % fluorapatite and in subsolidus regions in the presence of water, fluorapatite did not crystallize but fluorhydroxyapatite solid solutions coexisted with vapours containing up to 2.5 % hydrogen fluoride. These observations suggest that hydroxyapatite is more stable than fluorapatite at elevated temperatures and pressures and would be the composition expected to crystallize under igneous and metamorphic conditions.

THE common occurrence of fluorapatite in carbonatites and the association of fluorite with fluorapatite in carbonatite dykes, combined with recent experimental determination of phase equilibria in the systems $\text{CaO-CO}_2\text{-H}_2\text{O}$ (Wyllie and Tuttle, 1960), $\text{Ca}(\text{OH})_2\text{-CaF}_2\text{-CaCO}_3$ (Gittins and Tuttle, 1964), and $\text{CaO-P}_2\text{O}_5\text{-H}_2\text{O}$ (Biggar, 1966), have prompted a more complete investigation of the join $\text{Ca}(\text{OH})_2\text{-CaF}_2\text{-Ca}_3(\text{PO}_4)_2\text{-H}_2\text{O}$. Although fluorite is not abundant in carbonatites, von Eckermann (1948, pp. 124-40) records a number of dykes from Alnö with varying proportions of calcite, fluorite, and apatite. Dyke rocks consisting of up to 82 % fluorite and others with up to 20 % apatite were noted and Garson (1965) also records an apatite fluorite rock from Malawi. Von Eckermann (1961) stresses the possible importance of fluorine in carbonatite genesis. The join $\text{CaO-P}_2\text{O}_5\text{-H}_2\text{O}$ was chosen as a starting-point for an experimental study of some crystal-liquid reactions of possible relevance to carbonatites (Biggar, 1966) and with the addition of calcium fluoride to this join the experimental work

is improved in three respects: fluorapatite becomes a possible phase in addition to hydroxyapatite; a more complex liquid containing $\text{Ca}(\text{OH})_2$, CaF_2 , $\text{Ca}_3(\text{PO}_4)_2$, and H_2O is encountered thus bringing the composition of the experimental liquid closer to that believed to exist in carbonatite magma; and the phases fluorite and apatite may coexist with some of the liquids. If the liquids are regarded as simplified carbonatite magmas, then the solubility of apatite in them gives some indication of the range of apatite contents of natural carbonatites attributable to crystallization from a homogeneous liquid and consequently an indication of the range of apatite contents for which a process of crystal accumulation must be invoked.

By comparison with fluorapatite, hydroxyapatite occurs rarely in rocks and usually in assemblages in which water was abundant as deduced from the other phases present or in assemblages in which other minerals were in competition for the available fluorine. Several typical occurrences of hydroxyapatite in talc and chlorite schists are listed by Mitchell *et al.* (1943), and Vasileva (1957) gives examples of hydroxyapatites from low-temperature environments in which fluorine was deficient. There is a known preference for fluoride in aqueous solutions to concentrate in an apatite phase at low temperatures and pressures (Goldschmidt, 1954, p. 572) but the distribution of fluoride and hydroxyl ions between an apatite phase and any coexisting phase (solid, liquid, or vapour) has received little study at temperatures above 100°C and pressures above atmospheric. The experimental products were expected to include apatites equilibrated with calcium hydroxide and calcium fluoride in subsolidus regions, apatites equilibrated with liquids ranging in composition from calcium-hydroxide-rich to calcium-fluoride-rich, and apatites equilibrated in the presence of a vapour phase consisting primarily of water. Determination of the compositions of the apatites co-existing with these several phases may illuminate the factors that control the distribution of fluoride and hydroxyl ions between the apatite and the coexisting phases.

The experimental method. The experimental equipment, a description of the starting materials, and the techniques used for phase identification have been reported (Biggar, 1966). In addition the component calcium fluoride was required and material of more than 99.92% purity (supplied by Johnson, Matthey and Co.) was used.

The compositions experimentally studied lie within the system $\text{CaO}-\text{CaF}_2-\text{P}_2\text{O}_5-\text{H}_2\text{O}$ which is represented by the tetrahedron in fig. 1 and some of the compounds in the system are shown in weight %. The following abbreviations are used in the

text and figures: portlandite CH, fluorite CF, tricalcium phosphate C_3P , hydroxyapatite HA, fluorapatite FA, apatite solid solutions A or if known $\text{HA}_{30}\text{FA}_{70}$, liquid L, and vapour V. The experimental results are described with reference to the join $\text{CH-CF-FA-HA-H}_2\text{O}$, which is shown by the heavy lines in fig. 1. For the purposes of this paper the term stoichiometric apatite infers an apatite of the formula $\text{Ca}_{10}\text{P}_6\text{O}_{24}(\text{OH}, \text{F})_2$ and defect apatite infers any apatite for which there is experimental reason to suppose that the structure contains additional ions such as calcium

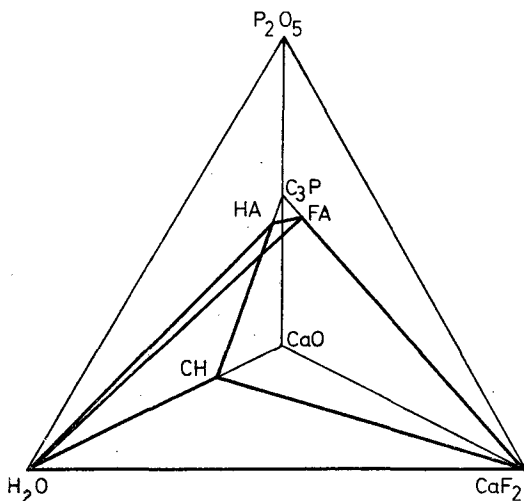


FIG. 1. Some of the compounds in the system $\text{CaO-CaF}_2\text{-P}_2\text{O}_5\text{-H}_2\text{O}$ in weight %. The abbreviations used are calcium hydroxide CH, calcium fluoride CF, hydroxyapatite HA, fluorapatite FA, tricalcium phosphate C_3P . The experimental results are described with reference to the join $\text{CH-CF-FA-HA-H}_2\text{O}$ which is shown by the heavy lines.

or additional molecules such as water. X-ray diffractometry was used to characterize the apatites and the most useful parameters were the position of the 140 and 231 diffraction peaks. For each apatite these peak positions were referred to the 311 peak of calcium fluoride as an internal standard, using $\text{Cu-K}\alpha$ radiation. Values of $\Delta 2\theta = 2\theta_{311}\text{CaF}_2 - 2\theta_{\text{apatite}}$ were determined for the 140 and 231 apatite peaks and were believed to be accurate to better than $\pm 0.02^\circ$.

Along with the phases described previously, fluorite was encountered as cubic crystals, which were somewhat rounded and were invariably so in the presence of vapour. These crystals increased in size in experiments at higher temperatures. The low index of refraction and isotropic nature of fluorite aided its identification. The quenched liquid resembled that previously described but in addition it contained dendrites of fluorite consisting of minute spherical particles regularly arranged in rows and columns and enclosed in quench portlandite.

Results. All diagrams and compositions are expressed in weight %. Compositions on the join $\text{CH-CF-FA-HA-H}_2\text{O}$ were studied at 1000 bars in the temperature range 600 to 950°C commencing with compositions

on the bounding joins FA-HA-H₂O and CH-CF-H₂O, and continuing with the 'dry' bounding join CH-CF-FA-HA, which was the join most extensively studied. Included in the experimental studies of this latter join are the determinations of apatite solid solution compositions and a description of miscellaneous experiments indicating that equilibrium was achieved. Of the remaining bounding joins, CH-HA-H₂O has been described (Biggar, 1966) and CF-FA-H₂O was not studied as it would yield no crystal-liquid equilibria at the temperatures attainable by the equipment. The experimental results for compositions on

TABLE I. The join FA-HA-H₂O at 1000 bars

Composition wt. %		Temp. ° C	Time days	Apatite		Result	
FA	H ₂ O			$\Delta 2\theta_{140}$	$\Delta 2\theta_{231}$	HA %	FA %
100	0	850	6½	4·16°	4·98°		100*
77	23	850	30	4·22	5·03	17	83
56	44	755	13	4·30	5·10	40	60
FA ₅₀ HA ₅₀							
75	25	850	30	4·39	5·18	66	34
50	50	755	13	4·45	5·23	82	18
HA							
100	0	850	6½	4·51	5·29	100*	
77	23	850	30	4·54	5·31		
53	47	755	13	4·54	5·31		

* Denotes reaction with the capsule.

the join CH-CF-FA-HA-H₂O are then described. In a final section on the effect of pressure some of the more important reactions encountered at 1000 bars are traced to higher and lower pressures.

The join FA-HA-H₂O. At 1000 bars pressure the beginning of melting of compositions on the join is above the temperature limit of the equipment but samples were maintained in the sub-solidus region. Dry charges crystallized as apatite but were discoloured (Biggar, 1966) and in charges with water present apatite crystals formed as pseudomorphs after the α -tricalcium phosphate starting material and only occasionally recrystallized to hexagonal prisms up to 0·03 mm long. The values of $\Delta 2\theta$ of the apatite products are listed in table I with, for ease of reference, some results previously reported (Biggar, 1966), and these increase progressively as water was added to each of the compositions FA, HA₅₀FA₅₀, and HA. For the first two compositions such a change in diffracted peak position may be entirely due to a reaction (hydrolysis) of the type fluorapatite and water giving hydroxyapatite and hydrogen

fluoride, $(x+y)\text{FA} + 2y\text{H}_2\text{O} \rightarrow \text{FA}_x\text{HA}_y + 2y\text{HF}$ yielding an hydroxy-fluorapatite solid solution of stoichiometric composition and a vapour containing H_2O and HF . The effect of water on the third composition, HA, was discussed (Biggar, 1966) and the formation of a defect apatite, with water in excess of that required by the formula, was postulated. By analogy, part of the change in the value of $\Delta 2\theta$ for the compositions FA and $\text{HA}_{50}\text{FA}_{50}$ may also be an effect of excess water in the structure.

These factors and the reaction of dry charges with the capsule make it impossible to use the results from the join FA-HA- H_2O to establish an accurate relationship between 2θ Δ and apatite composition. An approximate relationship would still be of value for determining approximate apatite compositions in joins of the type FA-HA-other-components and to obtain this approximation the discolouring reaction was assumed not to affect the angular position of the diffracted peaks and the effect of excess water in the structure was assumed to have little significant effect. The following linear relationships between mole % HA and $\Delta 2\theta$ were used: from table I, an apatite with $\Delta 2\theta_{140} = 4.16$ is FA and an apatite with $\Delta 2\theta_{140} = 4.51$ is HA and intermediate values of $\Delta 2\theta_{140}$ represent intermediate apatites on a linear basis. The values of $\Delta 2\theta_{231}$ are similarly treated, giving for each apatite two values of its composition and the arithmetic mean of these two values is quoted in determinations of apatite compositions. Since the molecular weights of hydroxy- and fluorapatite are so nearly identical, mole % and weight % are taken as identical and the results are expressed in weight %.

The above approximation is immediately useful for calculating the composition of the apatite in charges on the joins FA- H_2O and $\text{FA}_{50}\text{HA}_{50}\text{-H}_2\text{O}$. The charge with the bulk composition $\text{FA}_{56}(\text{H}_2\text{O})_{44}$ (table I) gave an apatite product which, from its $\Delta 2\theta$ value, calculated to the composition $\text{HA}_{40}\text{FA}_{60}$ and by a further calculation the vapour in equilibrium had the composition H_2O 98.4 HF 1.6. The other results of table I were similarly calculated and a plot of the apatite compositions and the calculated vapour compositions is shown in fig. 2. Compositions on the join FA-HA- H_2O are in equilibrium with vapours on the join $\text{H}_2\text{O}\text{-HF}$ (assuming negligible solubility of apatite in the vapour) and the pure fluorapatite end member did not form in the presence of water. Fig. 2 suggests that a vapour containing perhaps 3 % HF is necessary for the formation of fluorapatite in the temperature range 755-850° C at 1000 bars.

The join CH-CF- H_2O . The join CH-CF at 1000 bars has been reported by Gittins and Tuttle (1964) and the dashed lines in fig. 3 are from that report. The results for some experiments performed in the course of the present study are shown in fig. 3 and listed in table II. The solidus temperature, which is the temperature for the reaction $\text{CH} + \text{CF} \rightarrow \text{L}$, was found at 687° C (670° C reported by Gittins and Tuttle). The gradient of the fluorite liquidus differed slightly between

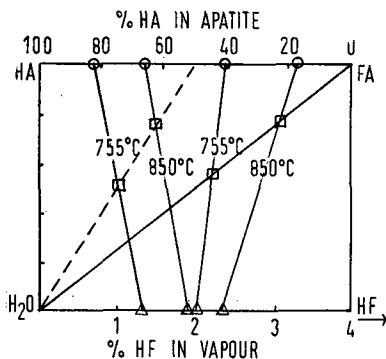
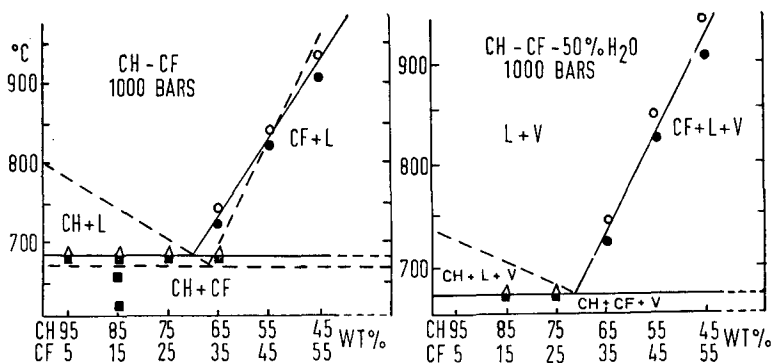


Fig. 2. Subsolidus results for the join FA-HA-H₂O at 1000 bars illustrating the departure of the vapour composition from pure water towards hydrogen fluoride. □ bulk compositions, ○ apatite compositions (determined by X-ray diffractometry), Δ vapour compositions (obtained by calculation).



Figs. 3 and 4: Fig. 3 (left). The join CH-CF at 1000 bars shown by the full lines. The dashed lines are the results published by Gittins and Tuttle, 1964. The reaction $\text{CH} + \text{CF} \rightarrow \text{L}$, E₄, occurs at 687° C and the liquid composition involved is CH₇₀CF₃₀. ○, L; Δ, CH+L; ●, CF+L; ■, subsolidus region, CH+CF. Fig. 4 (right). The section of the join CH-CF-H₂O at approximately 50% water at 1000 bars. The reaction $\text{CH} + \text{CF} + \text{V} \rightarrow \text{L}$, E₇, occurs at 675° C. ○, L+V; Δ, CH+L+V; ●, CF+L+V; ■, subsolidus region, CH+CF+V.

the two studies and the liquid composition involved in the reaction was CH₇₀CF₃₀ (Gittins and Tuttle reported CH₆₈CF₃₂).

The section of the join CH-CF-H₂O containing 50% water was experimentally studied and the results, shown in fig. 4, are listed in table II. The phases encountered were CH, CF, L containing calcium hydroxide plus calcium fluoride and water, and V consisting of almost

pure water. The temperature of the solidus, which is the reaction $\text{CH} + \text{CF} + \text{V} \rightarrow \text{L}$, was 675°C . It is seen from figs. 3 and 4 that the addition of water has little effect on the proportions of CH and CF in the liquid. The differences between figures such as that for the join CH-CF (fig. 3) and that for the section CH-CF-50 % H_2O (fig. 4) should

TABLE II. The join CH-CF- H_2O at 1000 bars

Composition			Temp. $^\circ\text{C}$ ± 5	Time d.h	Result			
ratio		wt. % H_2O			CH	CF	L	V
95	5			680	3.0	CH	CF	
		690		3.0	CH		L	
85	15		625	3.0	CH	CF		
			660	2.19	CH	CF		
			680	4.0	CH	CF		
			685	3.0	CH	CF		
			690	4.0	CH		L	
75	25		685	3.0	CH	CF		
			690	3.0	CH		L	
65	35		685	3.0	CH	CF		
			690	3.0		CF	L	
			725	2.0		CF	L	
			748	3.0			L	
55	45		825	3.0		CF	L	
			846	0.8			L	
45	55		910	0.5		CF	L	
			935	0.6			L	
85	15	50	670	3.0	CH	CF		V
		50	680	3.0	CH		L	V
75	25	50	670	2.0	CH	CF		V
		43	680	3.0	CH		L	V
65	35	48	725	3.0		CF	L	V
		50	748	3.0			L	V
55	45	51	830	0.7		CF	L	V
		50	850	0.7			L	V
45	55	47	910	0.7		CF	L	V
		51	945	0.3			L	V

be appreciated. The temperatures and bulk compositions at which phase changes occur can be read directly from both figures but only from figures for a join such as CH-CF can the liquid composition be read directly. Figures such as CH-CF-50 % H_2O , which represent sections through TX space, intersect phase volumes and the compositions of the phases are not directly obtainable. In the present case the liquid is water-poor (a value of 5 % water is assumed) and the vapour phase is water-rich (probably more than 99 % water). The two types of figure

are combined using the constructional methods described for the join $\text{CH}-\text{C}_3\text{P}-\text{H}_2\text{O}$ (Biggar, 1966) and the liquidus and vaporus field boundaries so obtained are shown in projection in fig. 5. The composition of the liquid involved in the reaction $\text{CH}+\text{CF}+\text{V} \rightarrow \text{L}$ at 675°C is estimated from fig. 5 as CH_{69} , CF_{26} , H_2O 5%. The temperatures of the reactions $\text{CH}+\text{CF} \rightarrow \text{L}$ and $\text{CH}+\text{CF}+\text{V} \rightarrow \text{L}$ at pressures other than 1000 bars are presented later.

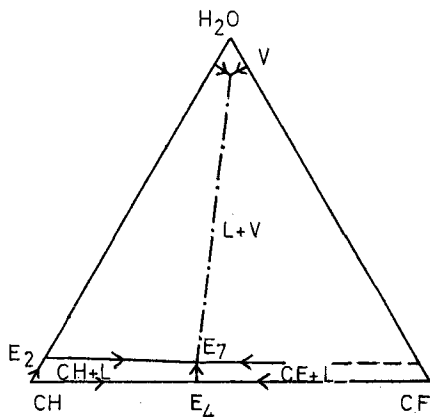


FIG. 5. Liquidus (true scale) and vaporus (distorted scale) field boundaries for the join $\text{CH}-\text{CF}-\text{H}_2\text{O}$ in projection at 1000 bars. The dash-dot line connects the coexisting liquid and vapour compositions for the reaction $\text{CH}+\text{CF}+\text{V} \rightarrow \text{L}$, E_7 , which occurs at 675°C . The liquid composition is estimated at $\text{CH}_{69}\text{CF}_{26}\text{H}_2\text{O}$ 5% and the vapour is almost pure water.

The join $\text{CH}-\text{CF}-\text{FA}-\text{HA}$ was determined in the temperature range $600-950^\circ\text{C}$ at 1000 bars by studying a selection of compositions lying on lines parallel to the join $\text{CH}-\text{CF}$ and containing 5%, 10%, 20%, and 30% C_3P . The experimental results obtained from these compositions are shown as isobaric TX sections in figs. 6-9 and the critical experiments used to determine the figures are listed in table III. The phases encountered were CH, CF, an apatite solid solution, and a liquid. In the TX sections through the join the temperature of the solidus, which is the reaction $\text{CH}+\text{CF}+\text{A} \rightarrow \text{L}$, was 675°C . On the 5% C_3P section the point at 740°C with the composition CH_{61} , CF_{34} , C_3P 5%, at which four phase-fields meet, is the piercing point of the fluorite-apatite liquidus field boundary. On the 10% C_3P section a piercing point at 955°C with the composition CH_{34} , CF_{56} , C_3P 10% was obtained by

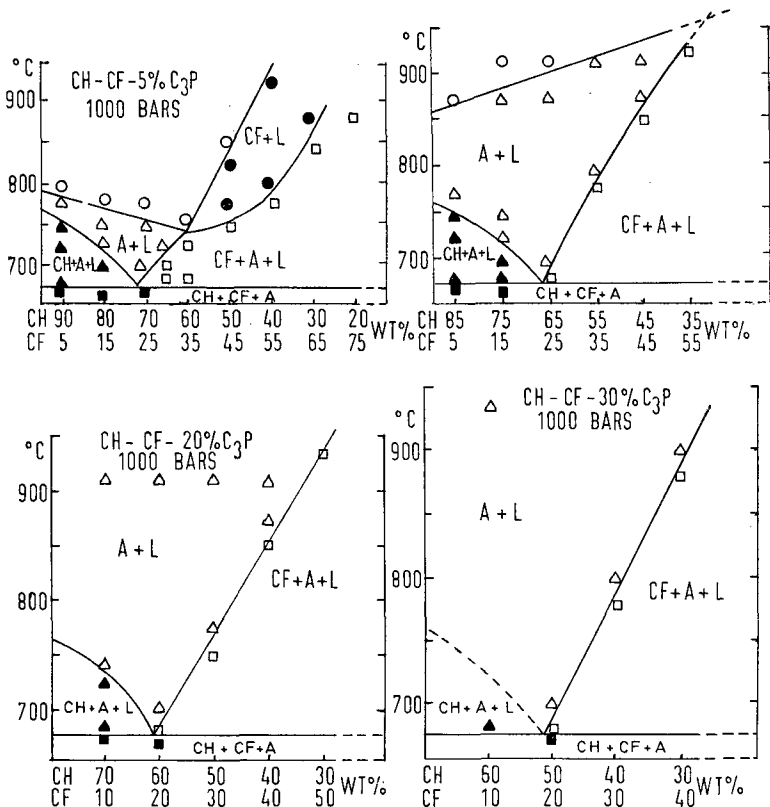
extrapolation. The complete, three-dimensional TX model of the phase relationships on the join CH-CF-FA-HA can be obtained by placing the experimentally determined TX sections in position in a TX prism and connecting the phase spaces and surfaces from one section to another.

TABLE III. The join CH-CF-FA-HA at 1000 bars

Composition					Time d.h.	Result			Composition										
wt. %			Temp. °C ±5			CH	CF	A	wt. %			Temp. °C ±5	Time dh.	Result					
CH	CF	C ₃ P			CH				CF	C ₃ P						CH	CF	A	L
90	5	5	670	3.0	CH	CF	A		75	15	10	700	3.0	CH		A	L		
			680	3.0	CH		A	L	725			3.0	CH		A	L			
			725	2.0	CH		A	L	750			4.0			A	L			
			750	3.0	CH		A	L	875			0.6			A	L			
			777	1.1			A	L	915			0.7			A	L			
80	15	5	798	3.0			A	L	65	25	10	682	3.0		CF	A	L		
			667	2.0	CH	CF	A	L	702			3.0			A	L			
			680	3.0	CH		A	L	875			0.6			A	L			
			700	3.0	CH		A	L	915			0.7			A	L			
			725	3.0	CH		A	L	775			4.0	CF		A	L			
70	25	5	750	3.0			A	L	55	35	10	798	3.0		CF	A	L		
			777	1.1			A	L	915			0.7			A	L			
			672	3.0	CH	CF	A	L	850			0.7		CF	A	L			
			682	3.0		CF	A	L	875			0.6			A	L			
			700	3.0			A	L	915			0.7			A	L			
65	30	5	750	3.0			A	L	35	55	10	925	0.6		CF	A	L		
			775	4.0			A	L	70			10	20	672	3.0	CH	CF	A	L
			682	3.0		CF	A	L	682			3.0	CH		A	L			
			700	3.0		CF	A	L	725			2.0	CH		A	L			
			725	3.0			A	L	740			3.0			A	L			
60	35	5	750	3.0			A	L	60	20	20	910	0.5		CH	CF	A	L	
			725	3.0	CF	A	L	667	2.0			CH	CF	A	L				
			750	3.0	CF	A	L	680	3.0			CF		A	L				
			775	4.0			A	L	700			3.0			A	L			
			682	3.0	CF	A	L	700	3.0					A	L				
50	45	5	825	3.0	CF	A	L	50	30	20	748	3.0		CF	A	L			
			850	3.0	CF		L	775			3.0			A	L				
			775	4.0	CF	A	L	910			0.5			A	L				
			800	3.0	CF		L	850			0.8	CF		A	L				
			925	0.6	CF		L	875			0.6			A	L				
40	55	5	845	0.8	CF	A	L	40	40	20	910	0.5			A	L			
			880	3.0	CF	A	L	910			0.5			A	L				
			880	3.0	CF	A	L	935			0.6			A	L				
			880	3.0	CF	A	L	30			50	20	935	0.6	CF	A	L		
			880	3.0	CF	A	L	60			10	30	680	3.0	CH		A	L	
30	65	5	670	3.0	CH	CF	A	50	20	30	935	0.6		CH		A	L		
			680	3.0	CH		A	L			670	3.0	CH	CF	A	L			
			725	2.0	CH		A	L			680	3.0		CF	A	L			
			750	4.0	CH		A	L			700	3.0			A	L			
			775	3.0			A	L			777	1.0		CF	A	L			
20	75	5	875	0.6			L	40	30	30	800	3.0			A	L			
			880	3.0	CH	CF	A	L			800	3.0			A	L			
			880	3.0	CH	CF	A	L			880	0.3		CF	A	L			
			880	3.0	CH	CF	A	L			900	0.5			A	L			
			880	3.0	CH	CF	A	L											

The geometry of these spaces and surfaces is more readily visualized by means of isothermal sections and a series of these is illustrated in fig. 10. The construction of isothermal sections from the experimentally determined TX sections follows the method described by Biggar (1966), and for the 800° C isothermal section (fig. 10B) crosses are shown to indicate data derived from the experimentally determined TX sections.

The liquid apices of the triangles $CF+A+L$, $CH+A+L$, and $CH+CF+L$ generate the liquidus field boundaries shown in projection in fig. 11. The three liquidus field boundaries meet at 675°C at a liquid composition CH_{73} , CF_{24} , C_3P 3%. The four phases CH , CF , A , and L coexist



FIGS. 6 TO 9: Fig. 6 (top left). The section $CH-CF-5\%$ C_3P at 1000 bars. \circ , L ; Δ , $A+L$; \bullet , $CF+L$; \blacktriangle , $CH+L$; \blacksquare , subsolidus region, $CH+CF+A+V$. FIG. 7 (top right). The section $CH-CF-10\%$ C_3P at 1000 bars; symbols as fig. 6. FIG. 8 (bottom left). The section $CH-CF-20\%$ C_3P at 1000 bars; symbols as fig. 6. FIG. 9 (bottom right). The section $CH-CF-30\%$ C_3P at 1000 bars; symbols as fig. 6.

at 675°C , which is the isobaric invariant temperature for the reaction $CH+CF+A \rightarrow L$. The apatite solid solution composition involved in the reaction is shown by the apatite end of the dash-dot line in fig. 11. The effect of changing pressure on the temperature of this reaction will be presented in a later section.

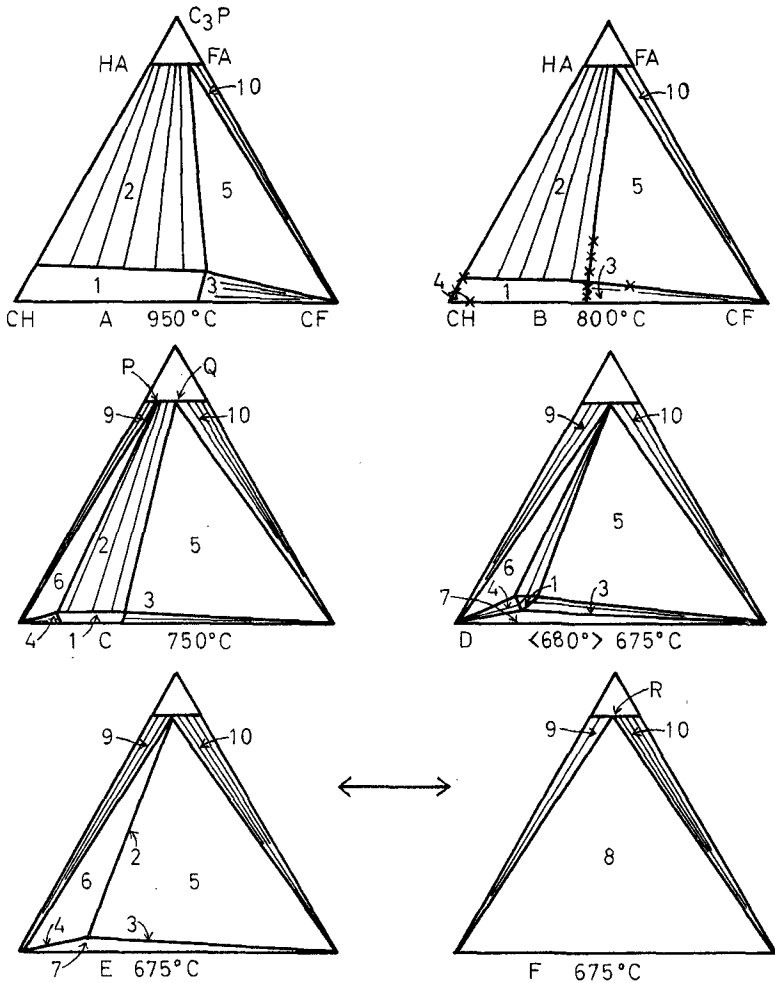
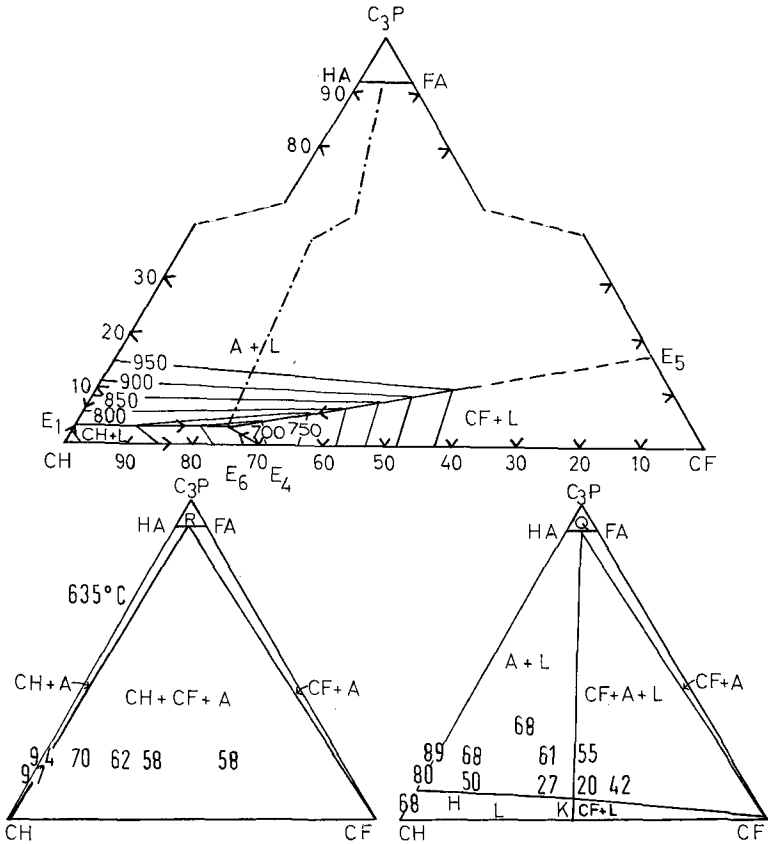


FIG. 10. Isothermal sections for the join CH-CF-FA-HA at 1000 bars. The experimentally determined points from which the sections are determined are illustrated as crosses in fig. 10B only. The phase fields are numbered as follows: 1, L; 2, A+L; 3, CF+L; 4, CH+L; 5, CF+A+L; 6, CH+A+L; 7, CH+CF+L; 8, CH+CF+A; 9, CH+A; 10, CF+A. The reaction $\text{CH}+\text{CF}+\text{A} \rightarrow \text{L}$, E_6 , is illustrated by figs. 10E and 10F and the liquid composition involved is $\text{CH}_{73}\text{CF}_{24}\text{C}_3\text{P} 3\%$.

In the isothermal sections shown in fig. 10 tie-lines in the two-phase fields are sketched in and only in the field A+L are they possibly of a different nature from those shown in the sketch. In fig. 10c two points along the join HA-FA are designated P and Q and in fig. 10f a point on the join HA-FA is designated R. These three points are apices of three phase triangles and represent the composition of the apatite solid solution that is in equilibrium with the other two phases at the temperature of the isothermal section. The compositions of the points P, Q, and R vary with temperature and their loci will be curves in a TX section. Since the A+L sides of the three phase triangles involving P and Q are also limiting case of tie-lines in the A+L field the determination of P and Q gives some indication of the nature of the tie-lines in the A+L field, which is in turn a measure of the partition of fluoride and hydroxyl ions between coexisting apatite and liquid phases. Three points on each of the limiting lines A+L are known from the experimentally determined TX sections at 10, 20, and 30 % C₃P. Extrapolation from these three points gives the apatite compositions P and Q, but the length of the extrapolation renders uncertain the compositions obtained by this method. Some evidence for the compositions of the points P, Q, and R on the join HA-FA is obtained from X-ray diffraction studies of selected charges and these results are now discussed.

X-ray diffraction patterns were obtained from selected charges to determine the compositions of the apatites in the charges and so to determine the positions of the points P, Q, and R at several temperatures. The apatite compositions were calculated as the arithmetic mean of the compositions obtained from the $\Delta 2\theta$ values as described in the section on the join HA-FA-H₂O. Charges at a temperature below 675° C represent the simplest case and the relevant isothermal section has been illustrated in fig. 10f. For the X-ray determinations charges were selected that had been equilibrated at a temperature of 635° C and those that lie within the three phase triangle CH-CF-R (fig. 10f) are expected to contain the one apatite with the composition that may be conveniently denoted R at 635° C. The experimental results for the apatite compositions are plotted in fig. 12 and range from 58 % to 70 % HA and there are two possible explanations for this discrepancy. It is known that on the join CH-C₃P (Biggar, 1966) the presence of calcium hydroxide influences the $\Delta 2\theta$ values of the apatite and this is emphasised by the values of 94 % and 97 % shown in fig. 12 but it is not known whether calcium fluoride has a similar or different effect. The range in values from 70 % to 58 % may reflect a change due



FIGS. 11 to 13: FIG. 11 (top). The join CH-CF-FA-HA in projection at 1000 bars showing liquidus field boundaries and thermal contours for liquidus surfaces. The dot-dash line connects the co-existing liquid and apatite solid solution compositions for the reaction $\text{CH} + \text{CF} + \text{A} \rightarrow \text{L}$, E_4 , which occurs at 675°C . FIG. 12 (bottom left). Apatite compositions on the 635°C isothermal section of the join CH-CF-FA-HA at 1000 bars determined by X-ray diffractometry (see text). The compositions are in wt % HA and are plotted on the bulk composition of the charge from which they are crystallized. FIG. 13 (bottom right). As for fig. 12 but for the 850°C isothermal section.

to the increasing calcium fluoride content of the charges. Alternatively, failure to achieve an equilibrium apatite solid solution at temperatures below the solidus may explain the discrepancy. Qualitatively the composition of the apatite may be placed at $65 \pm 10\%$ HA, which is richer in HA than might have been expected in the presence of excess calcium fluoride.

The phase relationships change considerably through the temperature range 675–800° C but above 800° C they are again simple enough (fig. 10B) to warrant an X-ray diffraction study of the apatites. Charges from a temperature of 850° C were selected and the determined apatite compositions are plotted in fig. 13 as % HA. The interpretation of fig. 13 is subject to considerable difficulties, the first of which is the presence of two apatites (primary and quench) in the same sample. With certain simplifying assumptions a qualitative picture of the apatite compositions in equilibrium in the several phase fields is obtainable. Charges in the liquid field precipitate apatite during the quench and those from liquids rich in portlandite (the region H, fig. 13) give an apatite with a composition of about 50 % HA as deduced from results in nearby phase fields where the quantity of contaminating primary apatite is small. Liquids containing about 50 % CH from the region K precipitate during the quench an apatite with a composition of about 20 % HA. Charges from the fields of A + L and CF + A + L contain two apatites (primary and quench) but the X-ray diffraction method does not necessarily reveal the mean apatite composition and in the present case almost certainly does not, due to the preferred orientation adopted by the acicular apatites during preparation of the sample for the X-ray diffractometer. Although a standard procedure was used for slide preparation profound changes in relative peak intensities were observed. At the 30 % C₃P composition line the weight ratio of primary to quench apatite is 5 to 1 and the results, to an approximation, may be taken as the values of the primary apatite composition. For these reasons the construction of reliable tie-lines in the field A + L and the accurate determination of the point Q at 850° C are not possible from the data but an estimate of Q at 850° C as greater than 62 % HA was made. Combining this value with the approximate value for R at 635° C the curves R and Q are plotted in fig. 14. No data for the curve P are available. With the above interpretation of the data of fig. 13 it should be noted that primary apatite in equilibrium with a liquid is richer in HA than the apatite produced during the rapid quench of the same liquid. At 850° C and 1000 bars a liquid of composition CH₄₇, CF₄₄, C₃P 8 % is in equilibrium with (is a saturated solution of) fluorite and an apatite of composition greater than 62 % HA. This slight enrichment of hydroxyl ion in the apatite relative to the liquid is very much the reverse of the effect of an aqueous liquid at normal temperatures and pressures. At temperatures above 850° C the liquid composition follows the fluorite-apatite field boundary, fig. 11, and the apatite composition follows the curve Q.

The attainment of equilibrium. Absolute proof that phase assemblages are stable rather than metastable is impossible since metastable assemblages can persist for great lengths of time and can undergo reversible changes. There are a number of experimental methods that subject the system to a more comprehensive range of time, temperature, and pressure variations and may eliminate obvious disequilibrium. In preliminary studies at temperatures below 800°C primary portlandite persisted

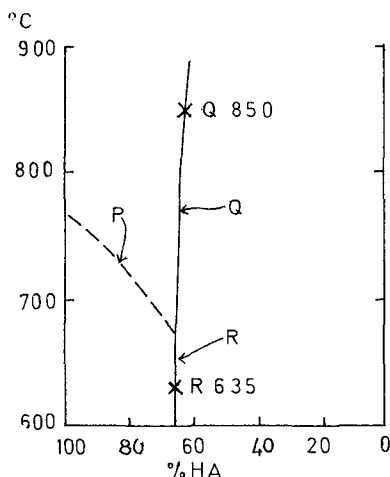


FIG. 14. The curves P, Q, and R are, respectively, the loci of the apatite compositions of the three-phase spaces $\text{CH}+\text{A}+\text{L}$, $\text{CF}+\text{A}+\text{L}$, and $\text{CH}+\text{CF}+\text{A}$ for the join CH-CF-FA-HA at 1000 bars.

metastably in experiments of less than 24 h duration and accordingly experiments of three or more days duration were chosen as standard below 800°C and were checked by a few experiments of thirty days duration. Above 800°C experiments of a few hours duration were identical with those of thirty days duration and the fact that data for the longer experiments fit smoothly on the data for shorter experiments is an indication that equilibrium exists.

Normally charges were raised without overshoot to the required temperature but as a check a selection of charges were taken to a higher temperature and a different phase field and held for three days to form the appropriate phase assemblage and subsequently lowered to the required temperature and maintained for three days prior to quenching. The result was invariably the assemblage stable at the lower temperature.

In the experiments so far described the apatite in the product crystallized from α -tricalcium phosphate in the starting material. Analysed natural fluorapatite from Dorowa (kindly given by Dr. R. L. Johnson and described by him, 1961) was mixed with 85 wt. % calcium hydroxide and, although the presence of impurities derived from the natural apatite render invalid any determination of solidus or liquidus temperatures, examination of samples maintained at 825° C and 1000 bars pressure revealed that the original fragments had recrystallized and that the primary and quench apatites formed had the characteristics of those derived from the usual starting material.

The X-ray diffraction data were:

natural apatite, $\Delta 2\theta_{140} = 4.33$, $\Delta 2\theta_{231} = 5.13$.

natural apatite plus 85 % CH, 825° C, 1000 bars, $\Delta 2\theta_{140} = 4.48$, $\Delta 2\theta_{231} = 5.23$.

This indicates a considerable increase in the hydroxyapatite content of the apatite solid solution. The same natural apatite when maintained at 840° C and 1000 bars for seven days in the presence of 50 % water gave a product for which $\Delta 2\theta_{140} = 4.42$, $\Delta 2\theta_{231} = 5.21$, indicating enrichment in hydroxyapatite. In neither case can the composition of the product be calculated because of impurities in the natural apatite but the enrichment is in agreement with the relationships shown in figs. 2 and 13. The formation of similar solid solution assemblages from different starting materials is an indication that equilibrium conditions obtain.

The quench method ceases to be valid for equilibrium determinations if any reaction rate is comparable with the quench rate. In the present system it seems unlikely that the exchange of hydroxyl ions in solution with fluoride ions in the apatite structure (or vice versa) will occur during the quench. There was no evidence of such a reaction when a slower quench rate was used but the criterion of a faster quench was impossible. (The normal quench rate involved cooling to 90° C in one minute.)

The join CH-CF-FA-HA-H₂O. The join was determined by studying a section at a constant water content. The tetrahedron CH-CF-C₃P-H₂O on which the join is represented is shown in fig. 15 and the dashed lines show the section containing 50 % water, which was selected for experimental study at 1000 bars. The results for compositions on this section that also contain C₃P as 10 % of the solids are shown in fig. 16 and listed in table IV. The phase fields intersected were CH+A+V, CF+A+L+V, A+L+V and L+V, and the solidus temperature was 665° C. A few experiments with compositions containing

20 and 30 % C_3P were performed, primarily to obtain apatite samples for comparisons (by X-ray diffractometer) with the 'dry' join CH-CF-FA-HA . There was no significant change in the apatite compositions in the presence of water.

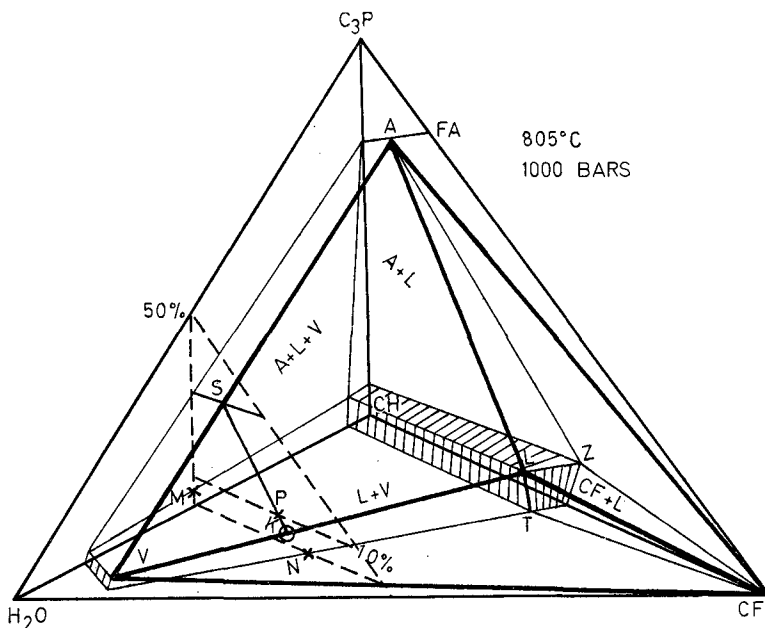


FIG. 15. Isothermal (805°C) tetrahedron for the join $\text{CH-CF-FA-HA-H}_2\text{O}$ at 1000 bars. The four-phase space CF+A+L+V is outlined in bold lines and the liquidus surfaces are shown shaded as is the one vaporus surface V(L) shown (on a distorted scale). The 50% water plane is lettered to correspond with fig. 17.

Comparison of the results for the section $\text{CH-CF-10\% C}_3\text{P-50\% H}_2\text{O}$ (fig. 16) with the results for the section $\text{CH-CF-10\% C}_3\text{P}$ (fig. 7) reveals that the addition of water produces little change in the form of the diagram and lowers by $10\text{-}40^\circ\text{C}$ the positions of comparable field boundaries. Similarly, comparison of the join CH-CF (fig. 3) with the section $\text{CH-CF-50\% H}_2\text{O}$ (fig. 4) shows a lowering of $5\text{-}15^\circ\text{C}$, and comparison of the join $\text{CH-C}_3\text{P}$ with the section $\text{CH-C}_3\text{P-50\% H}_2\text{O}$ (Biggar, 1966) shows a $10\text{-}30^\circ\text{C}$ lowering. With this small effect of water on the form of the diagrams and on temperatures it was considered unnecessary to perform further experiments on the join $\text{CH-CF-HA-FA-H}_2\text{O}$. To visualize the phase relationships on this join the construction of several

types of diagrams is helpful: The first, and simplest, is the isoplethal, isothermal section and as an example the section at 50% water and 805° C is illustrated in fig. 17 in which the crosses represent points taken from the experimentally determined diagrams. The cross at P is derived from fig. 16; the cross at N is taken from fig. 4; and the cross at M is

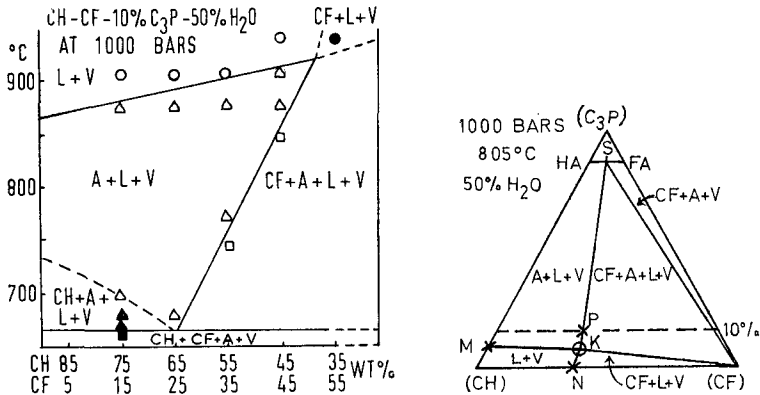
TABLE IV. The join CH-CF-FA-HA-H₂O at 1000 bars

Composition				Temp. °C	Time d. h	Result					
ratio			wt. %			±5					
CH	CF	C ₃ P	H ₂ O						L	V	
85	5	10	52	880	0.3						
75	15	10	47	660	2.19	CH	CF	A	L	V	
			49	670	3.0	CH		A	L	V	
			50	680	3.0	CH		A	L	V	
			51	700	2.19	CH		A	L	V	
			50	880	0.3			A	L	V	
			50	910	0.4				A	L	V
			46	680	3.0				A	L	V
65	25	10	47	880	0.3			A	L	V	
			49	910	0.4				L	V	
			50	748	3.0		CF	A	L	V	
55	35	10	51	775	4.0			A	L	V	
			50	880	0.3			A	L	V	
			48	910	0.4				L	V	
			51	850	0.7		CF	A	L	V	
45	45	10	47	880	3.0			A	L	V	
			52	910	0.4			A	L	V	
			49	945	0.3				L	V	
			52	945	0.3		CF		L	V	

taken from Biggar (1966). The point K, at which four phase-fields meet, was interpolated and at this point the phases CF and A just co-exist with L and V, indicating that the point lies on the L+V edge of the four-phase space CF+A+L+V.

To appreciate the value of isoplethal, isothermal sections their use in the construction of isothermal tetrahedra is discussed. The isothermal tetrahedron for the join CH-CF-FA-HA-H₂O at 805° C is shown in fig. 15 with some lines omitted for clarity. Previously determined isothermal planes for the bounding joins are drawn on the appropriate faces of the tetrahedron but the water apex and the apatite join are distorted to show more clearly the phase relationships. It is known that K lies on the L+V edge of the four-phase space CF+A+L+V and that the triangle K-S-(CF), fig. 17, is a section across this same space. The composition of the point V was not determined but it is believed

that the vapour is water-rich with only traces of other components dissolved in it (except for vapours close to the join $\text{FA-H}_2\text{O}$ for which a hydrogen fluoride content of the order of 2 % was demonstrated). The composition of the point L was not determined but a water content of less than 7.5 % is probable from the evidence of Wyllie and Tuttle (1960) and this view is reinforced by the small lowering of temperature caused



FIGS. 16 and 17: FIG. 16 (left). The section $\text{CH-CF-10 \% C}_3\text{P-50 \% H}_2\text{O}$ at 1000 bars. \circ , L+V ; \triangle , A+L+V ; \square , CF+L+V ; \blacktriangle , CH+L+V ; \blacksquare , $\text{subsolidus region, CH+CF+A+V}$. FIG. 17 (right). Isolethal (50 % H_2O) isothermal (805° C) section (not to scale) for the join $\text{CH-CF-FA-HA-H}_2\text{O}$ at 1000 bars. The crosses are from experimentally determined points and the parentheses emphasize that the apices are bulk compositions containing 50 % water.

by the presence of water. The four-phase space CF+A+L+V is drawn in and is shown by the bold lines in fig. 15. The remainder of the isothermal tetrahedron is constructed and the three liquidus surfaces are shown shaded. Only one vaporus surface V(L) is shown and it too is shaded while the other two vaporus surfaces V(CF) and V(A) are omitted. Tie-lines and tie-planes were not determined and are not shown in the isothermal tetrahedron. The two-phase spaces L+V , A+L , and CF+L , terminating on the shaded liquidus surfaces, contain tie-lines (not shown) as do the two-phase spaces CF+V and A+V , which would terminate on the omitted vaporus surfaces. Tie-planes exist in the three-phase spaces A+L+V and CF+A+L . In the isothermal tetrahedron illustrated there is one four-phase space CF+A+L+V shown by the bold lines, and the L and V corners of this generate, with changing temperature, the liquidus and vaporus field boundaries. On the apatite join, since the presence of water did not detectably alter the

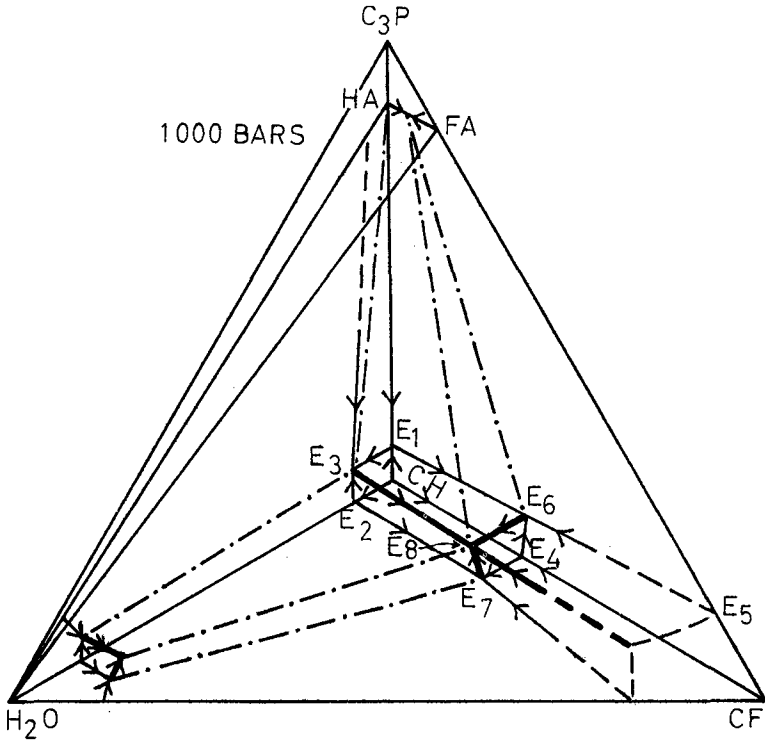


FIG. 18. The join CH-CF-FA-HA-H₂O at 1000 bars showing the liquidus and two of the three vaporus field boundaries on a distorted scale. The dot-dash lines connect co-existing phases, liquid, and vapour or liquid and apatite solid solution. The compositions of the liquids involved are: E₁, CH₉₆C₃P 4 %; E₂, CH₉₅H₂O 5; E₃, CH₉₂C₃P 4 H₂O 4; E₄, CH₇₀CF₃₀; E₅, unknown; E₆, CH₇₃CF₂₄C₃P 3; E₇, CH₆₉CF₂₆H₂O 5; E₈, CH₇₀CF₂₂C₃P 3 H₂O 5. The temperatures of the points are: E₁, 765° C; E₂, 785° C; E₃, 735° C; E₄, 687° C; E₅, unknown; E₆, 675° C; E₇, 675° C; E₈, 665° C.

apatite solid-solution compositions, the curves, P, Q, and R for the join CH-CF-FA-HA and a similar set of curves P', Q', and R' for the join CH-CF-FA-HA-H₂O are experimentally coincident, except that P, Q, and R meet at 675° C and P', Q', and R' meet at 665° C. In isothermal tetrahedra at lower temperatures (805-665° C) three other four-phase spaces are present CH+A+L+V, CH+CF+L+V, and CH+CF+A+L, which all contain portlandite as a phase and the corners of which generate field boundaries. These four four-phase spaces meet at the temperature 665° C and are replaced by the four-phase space CH+CF+A+V.

The four liquidus and two of the three vaporus field boundaries generated by the L and V apices of four-phase spaces (at temperature above 665° C) are shown in fig. 18 as bold lines and the previously determined field boundaries on the bounding joins are also shown. This figure summarizes the results of experiments at 1000 bars.

TABLE V. The join $\text{CH-CF-H}_2\text{O}$ at 250-4000 bars. Composition $\text{CH : CF} = 85 : 15$, anhydrous or with 48-51 wt. % H_2O

H_2O wt. %	Pressure	Temp.	Time d.h	Result				
	bars $\pm 5\%$	$^{\circ}\text{C}$ ± 5		CH	CF	L	V	
50	4000	645	0.6	CH	CF		V	
51	3850	655	0.6	CH		L	V	
	3900	670	0.5	CH	CF			
	4200	680	0.8	CH		L		
51	3000	640	1.6	CH	CF		V	
	48	3000	650	2.0	CH		L	V
		3050	670	3.0	CH	CF		
	3200	680	3.0	CH		L		
50	2000	650	2.8	CH	CF		V	
51	2000	660	3.0	CH		L	V	
	2000	680	3.0	CH	CF			
51	2000	690	3.0	CH		L		
	1000	See table II						
50	500	670	3.0	CH	CF		V	
48	500	680	3.0	CH		L	V	
	500	670	3.0	CH	CF			
	500	680	3.0	CH		L		
50	250	660	3.0	CH	CF		V	
50	250	670	3.0	CH		L	V	
	250	660	3.0	CH	CF			
	250	670	3.0	CH		L		

The effect of pressure. Two reactions that were encountered in the join $\text{CH-CF-H}_2\text{O}$ were experimentally determined at other pressures. The first reaction, $\text{CH} + \text{CF} \rightarrow \text{L}$, represents the beginning of melting of mixtures of portlandite and fluorite and the data are listed in table V and shown as a PT projection in fig. 19A. At a pressure of 500 bars the reaction was encountered at 675° C and the temperature rose to 687° C at 1000 bars and thereafter with a further increase in pressure a small drop in temperature was observed. This negative slope (dT/dP negative) above 1000 bars implies that the liquid is denser than the solids and as this is unlikely it appears that despite the precautions taken the charges picked up traces of water or carbon dioxide. Data for the reaction $\text{CH} + \text{CF} + \text{V} \rightarrow \text{L}$, representing the beginning of melting of compositions containing portlandite, fluorite, and water, are listed in

table V and shown in fig. 19A. At pressures between 500 and 2000 bars the temperature of the reaction decreases rapidly indicating an increased solubility of water in the liquid. The curves for both reactions, $\text{CH}+\text{CF}+\text{V} \rightarrow \text{L}$ and $\text{CH}+\text{CF} \rightarrow \text{L}$, intersect at some point between

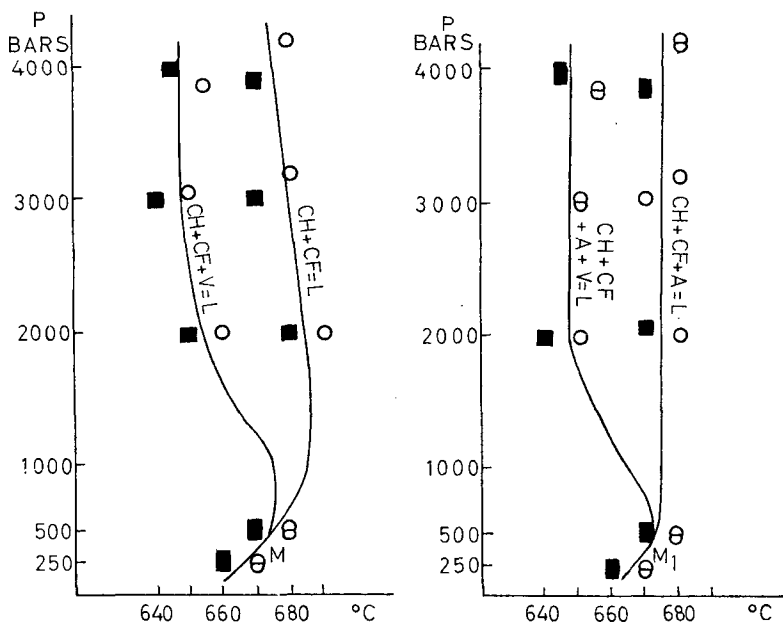


FIG. 19. A: The PT projections for the reactions $\text{CH}+\text{CF} \rightarrow \text{L}$ and $\text{CH}+\text{CF}+\text{V} \rightarrow \text{L}$ from 250 to 4000 bars. O, liquid present; \otimes , subsolidus region. B: The same for the reactions $\text{CH}+\text{CF}+\text{A} \rightarrow \text{L}$ and $\text{CH}+\text{CF}+\text{A}+\text{V} \rightarrow \text{L}$.

500 and 250 bars where the compositions of the liquids are identical. The liquid E_7 (fig. 5) then lies on the join $\text{CH}-\text{CF}$ and is identical with the liquid E_4 . At pressures below this point the two reactions are replaced by the reactions $\text{CH}+\text{CF} = \text{L}+\text{V}$ and mixtures on the join $\text{CH}-\text{CF}$ melt incongruently. To describe these phase relationships would require a discussion of the join $\text{CaO}-\text{CaF}_2-\text{H}_2\text{O}$.

The experimentally determined PT projections for the reactions $\text{CH}+\text{CF}+\text{A} = \text{L}$ and $\text{CH}+\text{CF}+\text{A}+\text{V} = \text{L}$ are very similar to the two just discussed and the data are collected in table V and plotted in fig. 19B. Where the curves meet between 250 and 500 bars the liquid compositions are identical and below this point the reaction $\text{CH}+\text{CF}+\text{A} \rightarrow \text{V}+\text{L}$ exists. The study of these four reactions over a

range of pressures provides data that can be used to assess the effects of pressure throughout the join $\text{CH-CF-HA-FA-H}_2\text{O}$. It is of particular interest to note the effects of changing pressure on liquid compositions, and, as an example of this effect, the probable change in the composition

TABLE VI. The join $\text{CH-CF-FA-HA-H}_2\text{O}$ at 250 to 4000 bars

Composition			wt. % H_2O	Pressure bars $\pm 5\%$	Temp. $^\circ\text{C}$ ± 5	Time d. h	Result			
CH	CF	C_3P					CH	CF	A	L
80	15	5	52	4000	645	0.6	CH	CF	A	V
75	15	10	49	4000	645	0.6	CH	CF	A	V
80	15	5	51	3850	655	0.6	CH		A	L V
75	15	10	48	3850	655	0.6	CH		A	L V
80	15	5	50	3000	640	1.6	CH	CF	A	V
75	15	10	49	3000	640	1.6	CH	CF	A	V
80	15	5	47	3090	650	2.0	CH		A	L V
75	15	10	49	3050	650	2.0	CH		A	L V
75	15	10	50	2000	640	3.0	CH	CF	A	V
75	15	10	50	2000	650	2.8	CH		A	L V
				1000			See table III			
80	15	5	50	500	670	3.0	CH	CF	A	V
75	15	10	51	500	680	3.0	CH		A	L V
80	15	5	50	250	660	3.0	CH	CF	A	V
75	15	10	50	250	670	3.0	CH		A	L V
80	15	5		3850	670	0.5	CH	CF	A	
75	15	10		3850	670	0.5	CH	CF	A	
80	15	5		4200	680	0.8	CH		A	L
75	15	10		4200	680	0.8	CH		A	L
80	15	5		3050	670	3.0	CH	CF	A	
80	15	5		3200	680	3.0	CH		A	L
80	15	5		2050	670	3.0	CH	CF	A	
75	15	10		2000	680	3.0	CH		A	L
				1000			See table III			
80	15	5		500	670	3.0	CH	CF	A	
75	15	10		500	680	3.0	CH		A	L
80	15	5		250	660	3.0	CH	CF	A	
75	15	10		250	670	3.0	CH		A	L

of the point L of fig. 15 is described. At pressures above 1000 bars the liquid is richer in water and the liquid field (the volume behind the shaded surfaces in fig. 15) expands towards the water apex. At some pressure between 500 and 250 bars the liquid composition, L, lies on the face $\text{CH-CF-C}_3\text{P}$ and at lower pressures the liquid lies within the join $\text{CaO-CH-CF-C}_3\text{P}$ and outside the scope of the present study. The temperatures of the reactions $\text{CH} + \text{CF} + \text{V} \rightarrow \text{L}$ and $\text{CH} + \text{CF} + \text{A} + \text{V} \rightarrow \text{L}$ differ by 10°C at 1000 bars but are not different, within the experimental limits, at pressures above 3000 bars (fig. 19). A possible

explanation of this effect is a decreased solubility of apatite in the liquid at elevated pressures and referring again to fig. 15 this infers that the liquid field contracts towards the base CH-CF-H₂O with increase in pressure.

Discussion and conclusions. If one accepts the assumptions involved in the interpretation of the X-ray data (which were that the $\Delta 2\theta$ value of an apatite from the join CH-CF-FA-HA was substantially a measure of the composition of the apatite between HA and FA and that the $\Delta 2\theta$ values of the end-members were based on values obtained from charges that had reacted slightly with the capsules) then the predominance with which hydroxyapatite-rich compositions (60 % HA) crystallized at 1000 bars in sub-solidus regions and from melts containing abundant calcium fluoride is the most unexpected aspect of the experimental studies. The synthesis of pure fluorapatite was not achieved in the presence of water and the trend of the apatite and vapour compositions plotted in fig. 2 suggest that some 3-4 % hydrogen fluoride in the vapour would be necessary for its formation at the temperatures and pressures concerned. The joins CH-CF-FA-HA and HA-FA-H₂O are simple systems compared with the geological environments from which natural apatites crystallize but these observations cast serious doubt on the greater stability of fluorapatite relative to hydroxyapatite at elevated pressure, suggesting rather the reverse. Further studies of the apatite compositions on the joins FA-HA-H₂O and CH-CF-FA-HA over a range of pressures would reveal if there was a progressive increase in stability of hydroxyapatite with increasing pressure. The X-ray diffraction data indicated that the compositions of apatites in the join CH-CF-FA-HA were not detectably altered by the addition of a water-rich vapour in the join CH-CF-FA-HA-H₂O and it should, further, be noted that although apatites crystallizing at equilibrium from liquids in the join CH-CF-FA-HA approximate to 60 % HA the same liquids on quenching yield apatite that is only 20 % HA; presumably the fluorapatite forms as a metastable phase during the quench. The experiments with the natural fluorapatite resulted in a defluorination of the original apatite. It would be of interest geologically and industrially to determine the threshold pressures and temperatures at which this type of reaction becomes significant.

Supporting field evidence for the formation of HA-rich compositions at elevated pressures, for example in carbonatites, is confused. Within a compilation of 139 apatite analyses taken from the literature and listed by Biggar (1962) there were six examples from carbonatites and ijolites,

although in not all of these cases did the authors, from the field evidence, ascribe a magmatic origin to the apatites:

1. Apatite from vermiculite apatite rock, Dorowa, Rhodesia. (Johnson, 1961); $\text{H}_2\text{O} + 0.16$, $\text{F} 3.38$, $\text{Cl} 0.10$ %.
2. Apatite from apatite rock, Kola, U.S.S.R. (Kind, 1939); $\text{H}_2\text{O} + 0.19$, $\text{F} 1.10$, $\text{Cl} 0.31$ %.
3. Apatite from ijolite, Iiwaara, Finland. (Kind, 1939); $\text{H}_2\text{O} + 0.54$, $\text{F} 1.83$, $\text{Cl} 0.13$ %.
4. Apatite, Kola, U.S.S.R. (Vlodavetz, 1939); $\text{H}_2\text{O} + 0.13$, $\text{F} 2.79$ %, Cl tr.
5. Apatite, Kola, U.S.S.R. (Vlodavetz, 1939); $\text{H}_2\text{O} + 0.28$, $\text{F} 1.97$, $\text{Cl} 0.09$ %.
6. Apatite from magnetite-apatite-phlogopite rock, Busumba, Uganda. (Davies, 1947); $\text{H}_2\text{O} + 0.98$, $\text{F} 2.26$ %.

The theoretical values for hydroxyapatite and fluorapatite are, respectively, 1.79 % H_2O and 3.77 % F and the above analyses can be recast in terms of the molecular proportions of HA and FA (neglecting the insignificant chlorine contents) to emphasize the confused nature of the results:

1. 9 HA 90 FA	3. 30 HA 49 FA	5. 16 HA 52 FA
2. 10 HA 29 FA	4. 7 HA 74 FA	6. 55 HA 60 FA

It is open to doubt whether even good apatite analyses will ever reveal the distribution of fluoride and hydroxyl ions in the original crystals since post-magmatic alteration of hydroxyapatite into fluorapatite at low temperature and pressure or by circulating aqueous solutions is such a probable geological process. If the greater stability of hydroxyapatite relative to fluorapatite is also true in silicate systems at elevated temperatures and pressures then hydroxyapatite may be the stable apatite of metamorphic rocks with again the probability of post-metamorphic conversion to fluorapatite (except in the fluorine-poor environments of certain talc and chlorite schists). In this connection experiments to ascertain the distribution of fluorine between apatite and fluorine-bearing silicate minerals at elevated temperatures and pressures would be of interest. On the basis of the results described here, it appears that there is a distinct possibility that hydroxyapatite is the common primary apatite of igneous and metamorphic rocks and that its abundance relative to that of fluorapatite increases with increase of pressure.

The experimental studies reveal that water has an insignificant effect

on the temperatures and liquid compositions of the several reactions that were determined. Only at pressures above 2000 bars does the presence of water lower temperatures by as much as 30° C and it is doubtful if there is any change in the CH:CF ratio of the liquid in the presence of water. Compared with the join CH-C₃P (Biggar, 1966) the present studies of the join CH-CF-FA-HA-H₂O extend the presence of liquids to temperatures as low as 645° C at 2000 bars. The solubility of apatite in these liquids remains low at 3 %, and apatite crystals settle out as described (Biggar, 1966). Liquids that on cooling are precipitating fluorite and apatite and coexist with a water-rich vapour undergo a variety of changes in composition in response to changes in pressure; above 2000 bars the liquid is relatively richer in dissolved water and perhaps poorer in dissolved apatite, becoming at lower pressures poorer in water and richer in apatite.

There is a need for more reliable data on natural apatite compositions and for more experimental work on joins such as $\text{CaCO}_3\text{-CaF}_2\text{-Ca}_3(\text{PO}_4)_2$ and $\text{CaCO}_3\text{-Ca}(\text{OH})_2\text{-Ca}_3(\text{PO}_4)_2$. The latter join is at present being studied and it is hoped that some information about carbonate-apatite will come from these studies. The need for experimental work to determine fluoride distribution between apatites and silicates has been mentioned.

Acknowledgements. The high pressure work was carried out in the School of Chemistry at Leeds University and the X-ray work in the Geology Department at Edinburgh University. The problem was suggested by P. J. Wyllie and his advice and that of R. S. Bradley during the research is gratefully acknowledged. The research at Leeds was supported by D.S.I.R. P. J. Wyllie very kindly reviewed drafts of the manuscript.

References

- BIGGAR (G. M.), 1962. Ph.D. Thesis, University of Leeds.
 — 1966. *Min. Mag.*, vol. 35, p. 1110.
 DAVIES (K. A.), 1947. *Econ. Geol.*, vol. 42, p. 137.
 VON ECKERMANN (H.), 1948. *Sver. Geol. Undersök.*, Ser. Ca., no. 36, 176 pp.
 — 1961. *Bull. Geol. Inst. Univ. Uppsala*, vol. 40, p. 25.
 GARSON (M. S.), 1965. *Bull. Geol. Surv. Malawi*, no. 15.
 GITTINS (J.) and TUTTLE (O. F.), 1964. *Amer. Journ. Sci.*, vol. 262, p. 66.
 GOLDSCHMIDT (V. M.), 1954. *Geochemistry*. Clarendon Press, Oxford.
 JOHNSON (R. L.), 1961. *Trans. Geol. Soc. South Africa*, vol. 64, p. 101.
 KIND (A.), 1939. *Chemie der Erde*, vol. 12, p. 50.
 MITCHELL (L.), FAUST (G. T.), HENDRICKS (S. B.), and REYNOLDS (D. S.), 1943. *Amer. Min.*, vol. 37, p. 656.
 VASILEVA (Z. V.) [Василева (З. В.)], 1957. *Geochemistry*, vol. 8, p. 825.
 VLONAVETZ (V. I.), 1939. *Amer. Min.*, vol. 24, p. 279.
 WYLLIE (P. J.) and TUTTLE (O. F.), 1960. *Journ. Petrology*, vol. 1, p. 1.

[Manuscript received 20 February 1967]